INTERNATIONAL SCIENTIFIC AND VOCATIONAL JOURNAL (ISVOS JOURNAL)

Vol.: 7 Issue: 2 Date: 31.12.2023 Received: 30.07.2023 Accepted: 10.12.2023 Final Version: 30.12.2023

ISVOS Journal, 2023, 7(2): 87-93 – DOI: 10.47897/bilmes.1334810

Estimation of Young's Modulus of Limestones using Multi-Layer Perceptron

Ebru Efeoğlu [a,1]

[a] Department of Sofrware Engineering, Engineering Faculty, Kütahya Dumlupınar University, Kütahya, Turkey
ORCID ID: 0000-0001-5444-6647

Abstract

The Young's modulus (E) is a very important parameter used in many engineering projects and in the petroleum industry. It is especially important for tunneling, mining and rock slope stability analysis. This parameter is determined by difficult experiments. In addition, cores must be taken for the experiment and the cores taken must be of high quality. The aim of the study is to estimate the Young's modulus, which represents the basic mechanical property of rocks, using relatively easy-to-apply and low-cost methods. For this purpose, the multi-layer perception method was used. Input parameters of these meshes are Dry density, Water saturated density, Bulk density, Porosity, Water absorption, Ultrasound Pulse Velocity (UPV), Poisson ratio (v), Tensile strength (To), The uniaxial compressive strength (UCS) and The point load index (Is)' is Four different network models were created and the successes of these network models were compared using the 5-fold cross-validation method. As a result of the comparison, it was understood that the model 2 network was more successful. The Correlation coefficient values of the model were calculated as 95% in training and 84% in 5-fold cross validation.

Keywords: "Artificial intelligence, multi-layer perceptron (MLP), Young's modulus, limestone, Spearman's rho, Kendall's Tau."

1. Introduction

Young's modulus (E), an important parameter for many engineering studies, reflects the hardness of rock materials. When a stress is applied to the rocks, deformation occurs in the rocks. This value is the ratio of this stress to the resulting deformation. The greater the value of the E value, the harder it is for the rocks to deform. Due to the difficulty of determining this parameter, limited budget and resources, researchers have searched for indirect methods to determine this parameter. In this study, some parameters of limestone collected from different regions of Turkey were used for the estimation of the E [1]. These parameters are Dry density, Water saturated density, Bulk density, Porosity, Is, Water absorption, UPV, Poisson ratio (v), tensile strength (To), and UCS. UPV determination method is a cheap, easy and reliable method. For this reason, it is often used to evaluate the mechanical properties of rocks. Another important parameter used in determining the mechanical properties of rocks is UCS. This parameter is widely used in engineering designs. It is a destructive method. In studies with the estimation of the mechanical properties of rocks, the UCS value has generally been estimated. For example, multivariate regression and LS-SVM methods [2], ANN method [3], PSO based artificial neural network (ANN) approach were used for UCS estimation [4]. UCS and E of intact sedimentary rocks using UPV were estimated using the least squares regression method [5]. Machine learning algorithms were used to estimate the E using the physical properties of rocks [6]. Least squares support vector machine based models were used to estimate the E of weak rocks [6]. The compressive strength of carbonate rocks was estimated [8]. M5P algorithm, which is one of the decision tree algorithms, was used to estimate the UCS value and the E of carbonate rocks. Schmidt hammer, porosity, dry unit weight and slake durability index were used as input variables to the algorithm [9]. Genetic algorithm was used for estimation of E [10]. The relationship of carbonate rocks with UCS value, density, E was investigated [11]. ANFIS and ICA methods were used to estimate the E of granite [12]. The unconfined compressive strength value and E values were estimated from the petrophysical properties of the carbonate rocks. Limestone, dolomite and chalk presented equations to estimate the Young's modulus (E) [13]. An XGBoost regression model was developed to estimate the E of sedimentary rocks [14]. In addition, linear-nonlinear regression analysis methods were used to estimate the E of thermally treated sedimentary rocks [15]. Deformation properties of charcoal were estimated by ANN and adaptive neuro-fuzzy inference system (ANFIS) method.

UCS, τ, shear strength and P wave velocity [16] were used as input parameters to the mesh. The estimation of UCS and E for travertine samples was made using the XGBoost algorithm [17]. Machine learning techniques were used to estimate the E of limestones [18]. Sawability of carbonate rocks was predicted from shear strength parameters with ANN [19]. Estimation of rock

[1] Corresponding Author
E-mail Address: ebru.efeoglu@dpu.edu.tr

properties using acoustic frequencies [20], rock fragmentation was estimated [21]. Machine learning based short term load forecasting was made in commercial buildings [22].

In this study, the Multi-Layer Perceptron (MLP) technique was used to estimate the Young modulus of limestones. To identify the network that made the most successful prediction, 4 different network models were created. Their prediction results were compared. Features used in the study are Dry density, Water saturated density, Bulk density, Porosity, Water absorption, Ultrasound Pulse Velocity (UPV), Poisson ratio (v), Tensile strength (To), The uniaxial compressive strength (UCS) and The point load index (Is). The histograms of the features in the data set used are given in Figure 1. Here, the vertical axis represents the frequency. Statistical parameters of the features were calculated and given in Table 1.

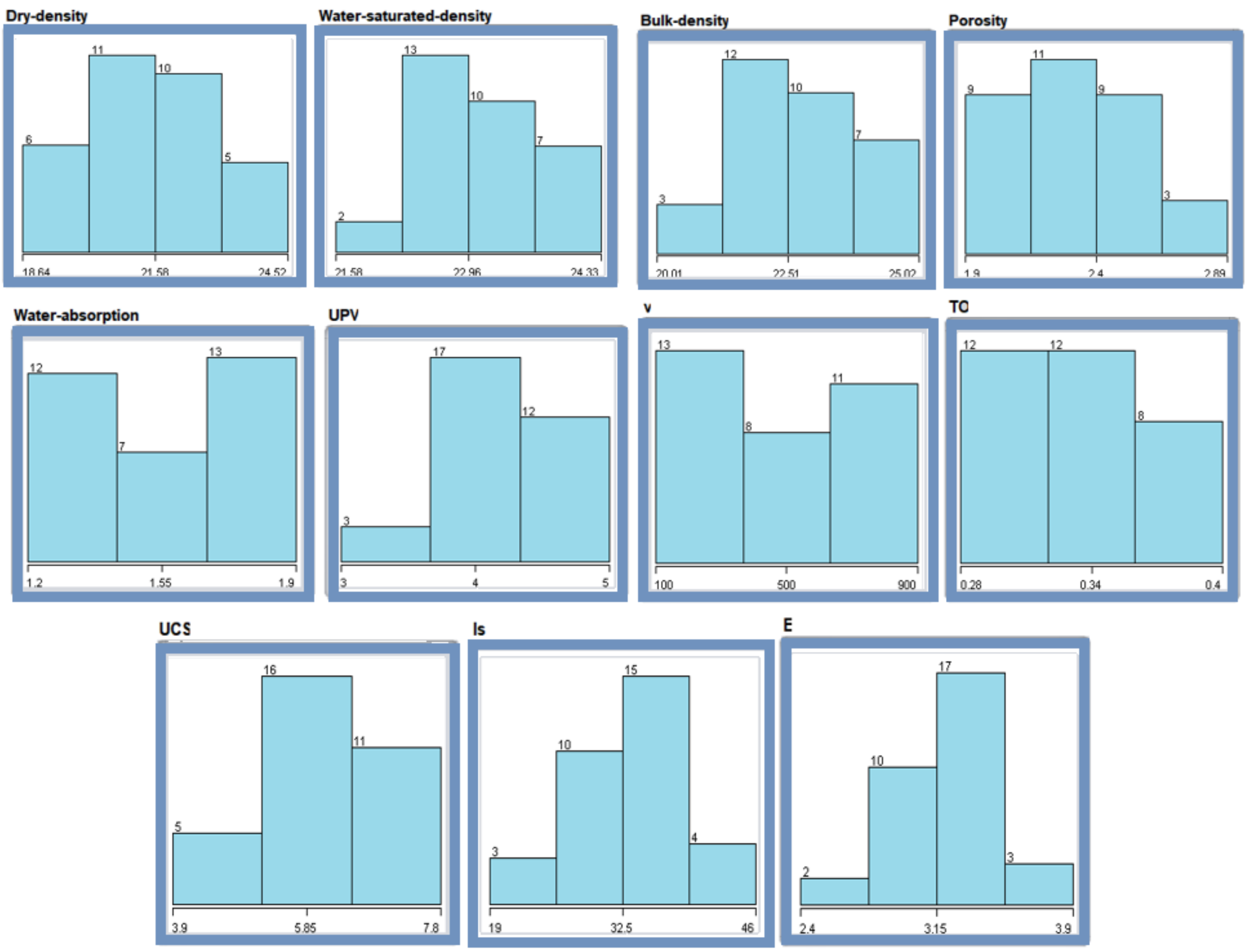

Fig 1. Histogram of the features

Table 1. Statistical parameters of the features

Features	Min	Max	Mean	StdDev
Dry- density	18.639	24.525	21.751	1.509
Water-saturated-density	21.582	24.329	23.078	0.667
Bulk-density	20.012	25.0.16	22.771	1.186
Porosity	1.9	2.89	2.313	0.236
Water-absorption	1.2	1.9	1.569	0.202
UPV	3478	5865	4766.25	556.212
V	0.28	0.4	0.339	0.033
To	3.9	7.8	6.15	1.099
UCS	19	46	33.156	6.248
Is	2.4	3.9	3.201	0.326
E	38.32	69.14	57.198	7.071

According to the table, the E varies between 38.32 and 69.14. The mean E value in the measurement data is 57.198 and the standard deviation is 7.071.

2. Materyal and Method

2.1. Multi-Layer Perceptron (MLP)

Multilayer perceptron model is used in case of non-linear relationships between inputs and outputs of ANN. MLP is a widely used ANN technique. This technique has a wide range of applications [21]. MLP's network consists of three layers. The network structure is given in Fig 2.

Input layer: ANN has inputs in this layer. There is no restriction on the number of entries. There is no information processing here. The information is sent to the next layer. Each process element in the input layer is connected to the process element in the next layer.

Hidden layer: Incoming information in this layer is processed and sent to the next layer. In an MLP network, there can be more than one middleware and more than one process element in each layer. Each process element in the middle layer is connected to the process element in the next layer.

Output layer: Here, it processes the information from the middleware and determines the outputs produced by the network in response to the inputs given to the network from the input layer. There can be more than one process element in this layer. Each process element is dependent on all the process elements in the previous layer. Each process element has only one output.

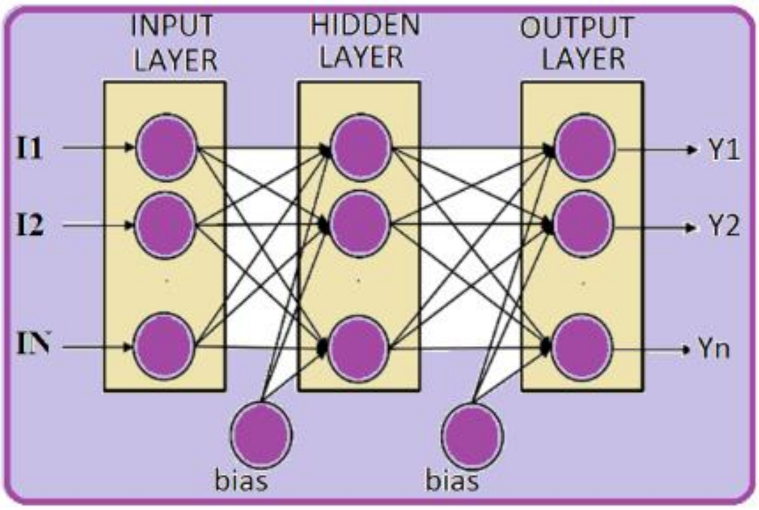

Fig. 2. MLP network

3. Results

In the study, 4 different network models were created for the estimation of the E. The same input parameters were used in all models. The first model consists of 1 hidden layer. There are 5 neurons in this layer. Model 2 has 2 hidden layers. There are 4 neurons in the first layer and 1 neuron in the second layer. Model-3 also has 2 hidden layers. There are 3 neurons in the first layer and 1 neuron in the second layer. Model 4 has 2 hidden layers. There are 2 neurons in the first layer and 1 neuron in the second layer.

The network models used, the inputs and outputs of the models, and the metrics used to compare their performance are given together. (Fig 3, Fig 4, Fig 5, Fig 6). In order to compare the models, Kendall' Tau, Spearman's rho, Correlation coefficient (R^2) and various error metrics used in the calculation of error values were calculated with weka. Kendall Tau identifies relationships between binary and ordinal scale data. If the Kendall's Tau coefficient is greater than 0.5, a high correlation is considered to exist. Kendall's Tau coefficient of all used models is higher than 0.5. But When this value is used in model 4, higher values were obtained than other models. The R^2 value is a value between -1 and +1. If R^2 is calculated as +1, there is a strong positive relationship between the two variables. If it is calculated as -1, there is a strong negative relationship. As this value approaches 0, the strength of the relationship weakens. This value was close to 1 in all networks. The highest values were obtained in Model 2 and Model 4. The highest value of R^2 is 0.95 in training and 0.84 in cross validation.In calculating the Spearman Rank Correlation Coefficient, the observation values are first ordered from the largest to the smallest or from the smallest to the largest, and a sequence number is given according to this order. If the Spearman Rank Correlation Coefficient is between 0.90 and 1, it means that there is a very strong relationship. The highest value was obtained when model 4 was used.

When the figures are examined, it is seen that the Spearman's rho, Kendall's Tau and R^2 of the model-4 are higher than the other models in both training and cross validation. In addition, the error metric values of this model are lower than other models. For this reason, it is appropriate to use the mesh structure created in Model-4 in estimating the Young's modulus.

Training

actual	predicted	error
64.36	52.991	-11.369
60.22	52.988	-7.232
59.44	52.986	-6.454
62.44	53.008	-9.432
52.2	52.961	0.761
62.46	53.003	-9.457
63	53.014	-9.986
58.44	52.985	-5.455
61.74	52.998	-8.742
65.32	52.993	-12.327
65	53.004	-11.996
62.7	52.995	-9.705
63.25	53.003	-10.247
60.34	52.987	-7.353
38.32	52.943	14.623
43.64	52.941	9.301
44.28	52.942	8.662
58.11	52.979	-5.131
54.3	52.98	-1.32
58.2	52.976	-5.224
59.36	52.97	-6.39
69.14	53.006	-16.134
55	52.98	-2.02
49.24	52.97	3.73
58.69	52.989	-5.701
55.7	52.971	-2.729
53.68	52.97	-0.71
65	52.984	-12.016
52.43	52.97	0.54
54	52.98	-1.02
49	52.965	3.965
51.34	52.973	1.633

5-fold cross validation

actual	predicted	error
44.28	48.645	4.365
51.34	51.391	0.051
58.69	59.227	0.537
65.32	63.102	-2.218
52.43	58.651	6.221
52.2	52.441	0.241
54	56.318	2.318
59.44	63.004	3.564
62.7	62.824	0.124
55	61.475	6.475
38.32	45.921	7.601
61.74	64.114	2.374
60.22	59.775	-0.445
55.7	55.744	0.044
63.25	62.378	-0.872
43.64	39.291	-4.349
54.3	62.725	8.425
49	52.548	3.548
62.46	62.017	-0.443
69.14	61.326	-7.814
58.2	53.724	-4.476
58.11	58.268	0.158
53.68	52.373	-1.307
65	61.695	-3.305
65	58.258	-6.742
59.36	65.006	5.646
60.34	65.958	5.618
63	69.486	6.486
62.44	69.465	7.025
58.44	59.167	0.727
64.36	62.588	-1.772
49.24	48.783	-0.457

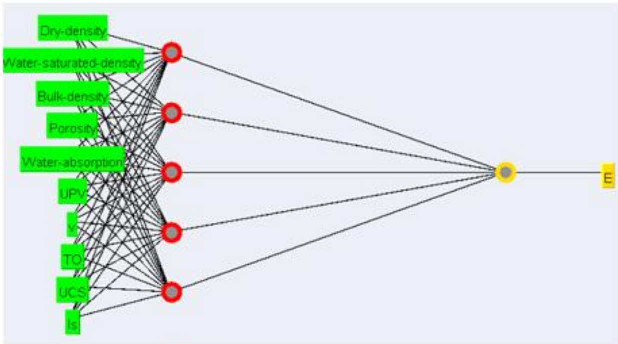

Training

Correlation coefficient	0.8986
Kendall's tau	0.7084
Spearman's rho	0.8791
Mean absolute error	6.9177
Root mean squared error	8.1234
Relative absolute error	122.3753 %
Root relative squared error	116.7201 %
Total Number of Instances	32

5-fold cross validation

Correlation coefficient	0.8183
Kendall's tau	0.5671
Spearman's rho	0.7442
Mean absolute error	3.3046
Root mean squared error	4.2867
Relative absolute error	56.7499 %
Root relative squared error	59.9357 %
Total Number of Instances	32

Fig. 3. Model-1 MLP network and its outputs

Training

actual	predicted	error
64.36	62.093	-2.267
60.22	61.166	0.946
59.44	59.753	0.313
62.44	64.452	2.012
52.2	50.68	-1.52
62.46	63.234	0.774
63	62.876	-0.124
58.44	56.611	-1.829
61.74	60.735	-1.005
65.32	62.447	-2.873
65	63.193	-1.807
62.7	61.324	-1.376
63.25	62.828	-0.422
60.34	59.12	-1.22
38.32	39.533	1.213
43.64	41.505	-2.135
44.28	43.476	-0.804
58.11	57.836	-0.274
54.3	56.887	2.587
58.2	54.62	-3.58
59.36	55.755	-3.605
69.14	63.56	-5.58
55	55.905	0.905
49.24	49.479	0.239
58.69	58.285	-0.405
55.7	54.429	-1.271
53.68	51.995	-1.685
65	57.345	-7.655
52.43	52.857	0.427
54	55.153	1.153
49	46.148	-2.852
51.34	49.422	-1.918

5-fold cross validation

actual	predicted	error
44.28	49.164	4.884
51.34	50.97	-0.37
58.69	58.3	-0.39
65.32	63.142	-2.178
52.43	56.819	4.389
52.2	50.709	-1.491
54	53.559	-0.441
59.44	61.087	1.647
62.7	62.391	-0.309
55	57.057	2.057
38.32	44.435	6.115
61.74	63.285	1.545
60.22	61.708	1.488
55.7	56.335	0.635
63.25	63.225	-0.025
43.64	42.023	-1.617
54.3	63.226	8.926
49	52.017	3.017
62.46	64.553	2.093
69.14	64.297	-4.843
58.2	52.008	-6.192
58.11	56.373	-1.737
53.68	50.402	-3.278
65	63.063	-1.937
65	57.185	-7.815
59.36	61.741	2.381
60.34	66.378	6.038
63	69.982	6.982
62.44	70.008	7.568
58.44	58.896	0.456
64.36	61.74	-2.62
49.24	49.034	-0.206

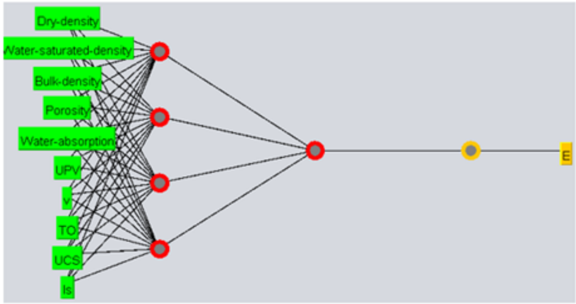

Training

Correlation coefficient	0.9536
Kendall's tau	0.7891
Spearman's rho	0.9202
Mean absolute error	1.7743
Root mean squared error	2.3741
Relative absolute error	31.3872 %
Root relative squared error	34.1117 %
Total Number of Instances	32

5-fold cross validation

Correlation coefficient	0.8455
Kendall's tau	0.6398
Spearman's rho	0.8157
Mean absolute error	2.9897
Root mean squared error	3.9188
Relative absolute error	51.342 %
Root relative squared error	54.7917 %
Total Number of Instances	32

Fig 4. Model-2 MLP network and its outputs

Training

actual	predicted	error
64.36	62.134	-2.226
60.22	61.442	1.222
59.44	59.862	0.422
62.44	64.666	2.226
52.2	50.879	-1.321
62.46	63.29	0.83
63	63.018	0.018
58.44	56.19	-2.25
61.74	60.79	-0.95
65.32	62.757	-2.563
65	63.278	-1.722
62.7	61.348	-1.352
63.25	63.08	-0.17
60.34	59.08	-1.26
38.32	39.523	1.203
43.64	41.527	-2.113
44.28	43.627	-0.653
58.11	58.086	-0.024
54.3	57.001	2.701
58.2	54.599	-3.601
59.36	55.57	-3.79
69.14	63.536	-5.604
55	56.159	1.159
49.24	49.407	0.167
58.69	58.389	-0.301
55.7	54.59	-1.11
53.68	51.989	-1.691
65	57.603	-7.397
52.43	53.068	0.638
54	55.298	1.298
49	46.187	-2.813
51.34	49.236	-2.104

5-fold cross validation

actual	predicted	error
44.28	48.931	4.651
51.34	50.478	-0.862
58.69	59.018	0.328
65.32	63.701	-1.619
52.43	57.658	5.228
52.2	50.898	-1.302
54	53.917	-0.083
59.44	61.657	2.217
62.7	62.508	-0.192
55	57.277	2.277
38.32	44.549	6.229
61.74	64.206	2.466
60.22	62.305	2.085
55.7	57.346	1.646
63.25	62.866	-0.384
43.64	40.416	-3.224
54.3	62.722	8.422
49	52.301	3.301
62.46	63.773	1.313
69.14	63.629	-5.511
58.2	51.617	-6.583
58.11	56.414	-1.696
53.68	50.353	-3.327
65	61.766	-3.234
65	58.374	-6.626
59.36	64.719	5.359
60.34	66.585	6.245
63	69.908	6.908
62.44	69.988	7.548
58.44	58.969	0.529
64.36	61.728	-2.632
49.24	48.712	-0.528

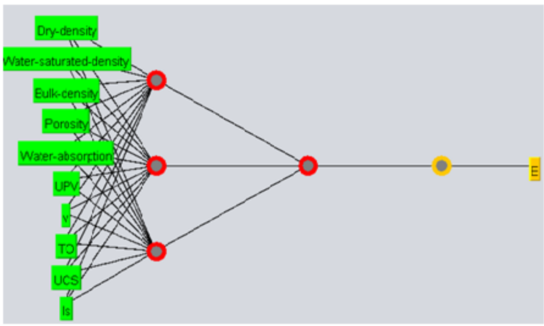

Training

Correlation coefficient	0.9518
Kendall's tau	0.7891
Spearman's rho	0.9187
Mean absolute error	1.7781
Root mean squared error	2.3719
Relative absolute error	31.4543 %
Root relative squared error	34.0805 %
Total Number of Instances	32

5-fold cross validation

Correlation coefficient	0.8387
Kendall's tau	0.6075
Spearman's rho	0.7957
Mean absolute error	3.2673
Root mean squared error	4.0782
Relative absolute error	56.1097 %
Root relative squared error	57.0204 %
Total Number of Instances	32

Fig 5. Model-3 MLP network and its outputs

Training

actual	predicted	error
64.36	62.248	-2.112
60.22	61.686	1.466
59.44	59.993	0.553
62.44	65.19	2.75
52.2	50.957	-1.243
62.46	63.491	1.031
63	63.462	0.462
58.44	56.113	-2.327
61.74	60.976	-0.764
65.32	63.16	-2.16
65	63.665	-1.335
62.7	61.634	-1.066
63.25	63.639	0.389
60.34	59.313	-1.027
38.32	39.03	0.71
43.64	42.081	-1.559
44.28	43.562	-0.718
58.11	57.859	-0.251
54.3	57.386	3.086
58.2	54.662	-3.538
59.36	55.514	-3.846
69.14	63.909	-5.231
55	56.309	1.309
49.24	49.258	0.018
58.69	58.726	0.036
55.7	54.934	-0.766
53.68	52.623	-1.057
65	57.887	-7.113
52.43	53.522	1.092
54	55.762	1.762
49	46.073	-2.927
51.34	49.319	-2.021

5- fold cross validation

actual	predicted	error
44.28	48.528	4.248
51.34	50.32	-1.02
58.69	59.135	0.445
65.32	63.591	-1.729
52.43	57.713	5.283
52.2	49.731	-2.469
54	51.983	-2.017
59.44	61.172	1.732
62.7	61.728	-0.972
55	57.365	2.365
38.32	43.12	4.8
61.74	62.777	1.037
60.22	61.525	1.305
55.7	55.954	0.254
63.25	63.91	0.66
43.64	44.094	0.454
54.3	63.374	9.074
49	53.057	4.057
62.46	64.686	2.226
69.14	64.992	-4.148
58.2	51.295	-6.905
58.11	56.572	-1.538
53.68	50.056	-3.624
65	64.144	-0.856
65	56.518	-8.482
59.36	60.311	0.951
60.34	66.83	6.49
63	69.965	6.965
62.44	70	7.56
58.44	58.807	0.367
64.36	61.936	-2.424
49.24	49.856	0.616

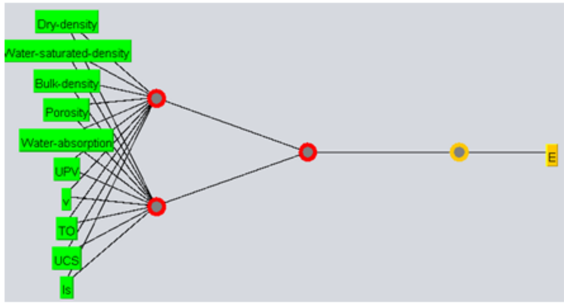

Training

Correlation coefficient	0.951
Kendall's tau	0.7931
Spearman's rho	0.9227
Mean absolute error	1.7414
Root mean squared error	2.3099
Relative absolute error	30.8059 %
Root relative squared error	33.1902 %
Total Number of Instances	32

5- fold cross validation

Correlation coefficient	0.8421
Kendall's tau	0.672
Spearman's rho	0.8265
Mean absolute error	3.0336
Root mean squared error	3.9856
Relative absolute error	52.0966 %
Root relative squared error	55.7255 %
Total Number of Instances	32

Fig 6. Model-4 MLP network and its outputs

References

[1] Kurtulus, C., Cakir, S., & Yoğurtcuoğlu, A.C. "Ultrasound Study of Limestone Rock Physical and Mechanical Properties". Soil Mechanics & Foundation Engineering, 52(6), 2016.

[2] Çelik SB. "Prediction of uniaxial compressive strength of carbonate rocks from nondestructive tests using multivariate regression and LS-SVM methods". Arab J Geosci 2019;12:193. https://doi.org/10.1007/s12517-019-4307-2.

[3] Ferentinou M, Fakir M. "An ANN Approach for the Prediction of Uniaxial Compressive Strength, of Some Sedimentary and Igneous Rocks in Eastern KwaZulu-Natal". Symposium of the International Society for Rock Mechanics 2017, 191:1117–25. https://doi.org/10.1016/j.proeng.2017.05.286.

[4] Mohamad ET, Jahed Armaghani D, Momeni E, Alavi Nezhad Khalil Abad SV. "Prediction of the unconfined compressive strength of soft rocks: a PSO-based ANN approach". Bull Eng Geol Environ 2015;74:745–57.

[5] Z.A. Moradian, M. Behnia, "Predicting the uniaxial compressive strength and static Young's modulus of intact sedimentary rocks using the ultrasonic test".Int. J. Geomech. 9 (1(14)) 1532–3641, 2009.

[6] Khan, N. M., Cao, K., Yuan, Q., Bin Mohd Hashim, M. H., Rehman, H., Hussain, S., ... & Khan, S. "Application of machine learning and multivariate statistics to predict uniaxial compressive strength and static Young's modulus using physical properties under different thermal conditions". Sustainability, 14(16), 9901,2022.

[7] Acar, M. C., & Kaya, B. "Models to estimate the elastic modulus of weak rocks based on least square support vector machine". Arabian Journal of Geosciences, 13(14), 590, 2020.

[8] Madhubabu, N., Singh, P. K., Kainthola, A., Mahanta, B., Tripathy, A., & Singh, T. N. "Prediction of compressive strength and elastic modulus of carbonate rocks". Measurement, 88, 202-213, 2016.

[9] Ghasemi, E., Kalhori, H., Bagherpour, R., & Yagiz, S. "Model tree approach for predicting uniaxial compressive strength and Young's modulus of carbonate rocks". Bulletin of Engineering Geology and the Environment, 77, 331-343., 2018.

[10] E. Yasar, Y. Erdogan, "Correlating sound velocity with the density, compressive strength and Young's modulus of carbonate rocks". Int. J. Rock Mech. Min. Sci. 41 871, 2004.

[11] Armaghani, D.J., Tonnizam Mohamad, E., Momeni, E., Monjezi, M., Narayanasamy, M.S., 2016. "Prediction of the strength and elasticity modulus of granite through an expert artificial neural network". Arabian Journal of Geosciences 9 (48), 1e16

[12] Hadi, F., & Nygaard, R. Estimating unconfined compressive strength and Young's modulus of carbonate rocks from petrophysical properties. Petroleum Science and Technology, 41(13), 1367-1389,2023.

[13] Shahani, N. M., Zheng, X., Liu, C., Hassan, F. U., & Li, P. "Developing an XGBoost regression model for predicting young's modulus of intact sedimentary rocks for the stability of surface and subsurface structures". Frontiers in Earth Science, 9, 761990, 2021.

[14] Waqas, U., & Ahmed, M. F. "Prediction modeling for the estimation of dynamic elastic Young's modulus of thermally treated sedimentary rocks using linear–nonlinear regression analysis, regularization, and ANFIS". Rock Mechanics and Rock Engineering, 53, 5411-5428, 2020.

[15] Roy, D. G., & Singh, T. N. "Predicting deformational properties of Indian coal: Soft computing and regression analysis approach". Measurement, 149, 106975, 2020.

[16] Nasiri, H., Homafar, A., & Chelgani, S. C. "Prediction of uniaxial compressive strength and modulus of elasticity for Travertine samples using an explainable artificial intelligence". Results in Geophysical Sciences, 8, 100034, 2021.

[17] Mahmoud, A. A., Elkatatny, S., & Al Shehri, D. "Application of machine learning in evaluation of the static young's modulus for sandstone formations". Sustainability, 12(5), 1880, 2020.

[18] Kahraman, S. A. İ. R., Altun, H., Tezekici, B. S., & Fener, M. "Sawability prediction of carbonate rocks from shear strength parameters using artificial neural networks". International journal of rock mechanics and mining sciences, 43(1), 157-164, 2006.

[19] Kumar, C. V., Vardhan, H., & Murthy, C. S. "Artificial neural network for prediction of rock properties using acoustic frequencies recorded during rock drilling operations". Modeling Earth Systems and Environment, 8(1), 141-161, 2022.

[20] Ebrahimi, E., Monjezi, M., Khalesi, M. R., & Armaghani, D. J. "Prediction and optimization of back-break and rock fragmentation using an artificial neural network and a bee colony algorithm". Bulletin of Engineering Geology and the Environment, 75, 27-36, 2016.

[21] Lu, S., Koopialipoor, M., Asteris, P. G., Bahri, M., & Armaghani, D. J. "A novel feature selection approach based on tree models for evaluating the punching shear capacity of steel fiber-reinforced concrete flat slabs". Materials, 13(17), 3902., 2020.

[22] Erten, M.Y., İnanç, N.. "Machine Learning Based Short Term Load Estimation in Commercial Buildings". ISVOS. 5:171–181, 2021.